A generic multivariate framework for the integration of microbiome longitudinal studies with other data types

Antoine Bodein [1†], Olivier Chapleur [2†], Arnaud Droit [1], Kim-Anh Lê Cao [3,∗]

[1]CHU de Québec Research Center, Université Laval, Molecular Medicine department, Québec, QC, Canada,

[2] Hydrosystems and Bioprocesses Research Unit, Irstea, Antony , France,

[3]Melbourne Integrative Genomics, School of Mathematics and Statistics, University of Melbourne, Melbourne, VIC, Australia

[†] Both authors contributed equally to this manuscript

March 21, 2019

Abstract

Simultaneous profiling of biospecimens using different technological platforms enables the study of many data types, encompassing microbial communities, omics and meta-omics as well as clinical or chemistry variables. Reduction in costs now enables longitudinal or time course studies on the same biological material or system. The overall aim of such studies is to investigate relationships between these longitudinal measures in a holistic manner to further decipher the link between molecular mechanisms and microbial community structures, or host-microbiota interactions. However, analytical frameworks enabling an integrated analysis between microbial communities and other types of biological, clinical or phenotypic data are still at their infancy. The challenges include few time points that may be unevenly spaced and unmatched between different data types, a small number of unique individual biospecimens and high individual variability. Those challenges are further exacerbated by the inherent characteristics of microbial communities-derived data (e.g. sparsity, compositional).

We propose a generic data-driven framework to integrate different types of longitudinal data measured on the same biological specimens with microbial communities data, and select key temporal features with strong associations at the sample group level. The framework ranges from filtering and modelling, to integration using smoothing splines and multivariate dimension reduction methods to address some of the analytical challenges of microbiome-derived data. We illustrate our framework on different types of multi-omics case studies in bioreactor experiments as well as human studies.

Keywords: Time course, data integration, splines, feature selection

1 Introduction

Microbial communities are highly dynamic biological systems that cannot be fully investigated in snapshot studies. The decreasing cost of DNA sequencing has enabled longitudinal and time-course studies to record the temporal variation of microbial communities (Faust *et al.*, 2015; Knight *et al.*, 2012). These studies can inform us about the stability and dynamics of microbial communities in response to perturbations or different conditions of the host or their habitat and can capture the dynamics of microbial interactions (Ridenhour *et al.*, 2017; Bucci *et al.*, 2016) or associate change of microbial features, such as taxonomies or genes, to a phenotypic group (Metwally *et al.*, 2018).

However, besides the inherent characteristics of microbiome data, including sparsity, compositionality (Aitchison, 1982; Gloor *et al.*, 2017), its multivariate nature and high variability (Lê Cao *et al.*, 2016b), longitudinal studies suffer from irregular sampling and subject drop-outs. Thus, appropriate modelling of the microbial profiles is required, for example by using splines modelling. Methods including loess (Shields-Cutler *et al.*, 2018), smoothing spline ANOVA (Paulson *et al.*, 2017), negative binomial smoothing splines (Metwally *et al.*, 2018) or gaussian cubic splines (Luo *et al.*, 2017) were proposed to model

---

∗Corresponding Author: kimanh.lecao@unimelb.edu.au

dynamics of microbial profiles across groups of samples or subjects. The aim of these approaches is to make statistical inferences about global changes of differential abundance across multiple phenotypes of interest, rather than at specific time points. These proposed methods are univariate, and as such, cannot infer ecological interactions (Morris *et al.*, 2016). Other types of methods aim to cluster microbial profiles to posit hypotheses about symbiotic relationships, interaction or competition. For example Baksi *et al.* (2018) used a Jenson Shannon Divergence metric to visually compare metagenomic time series.

Multivariate ordination methods can exploit the interaction between microorganisms, but need to be used with sparsity constraints, such as ℓ_1 regularization (Tibshirani, 1996), to reduce the number of variables and improve interpretability through variable selection. Several sparse methods were proposed and applied to microbiome studies, such as sparse linear discriminant analysis (Clemmensen *et al.*, 2011) and sparse Partial Least Squares Discriminant Analysis (sPLS-DA, Lê Cao *et al.* 2016a), but for a single time point. Therefore, further developments are needed to combine both time-course modelling with multivariate approaches to start exploring microbial interactions and dynamics.

In addition, current statistical methods have mainly focused on a single microbiome dataset, rather than the combination of different layers of molecular information obtained with parallel multi-omics assays performed on the same biological samples. Data derived from each omics technique are typically studied in isolation, and disregard the correlation structure that may be present between the multiple data types. Hence, integrating these datasets enable us to adopt a holistic approach to elucidate patterns of taxonomic and functional changes in microbial communities across time. Some sparse multivariate methods have been proposed to integrate omics and microbiome datasets at a single time point and identify sets of features (multi-omics signatures) across multiple data types that are correlated with one another. For example, Gavin *et al.* (2018) used the DIABLO method (Singh *et al.*, 2019) to integrate 16S, proteomics and metaproteomics in a type I diabetes study, Guidi *et al.* (2016) used sparse PLS (Lê Cao *et al.*, 2008) to integrate environmental and metagenomic data from the Tara Oceans expedition to understand carbon export in oligotrophic oceans, and Fukuyama *et al.* (2017) used sparse Canonical Correlation Analysis (Witten *et al.*, 2009) to integrate 16S and metagenomic data. However, methods or frameworks to integrate multiple longitudinal datasets including microbiome data remain incomplete. To our knowledge, only one study (Ribicic *et al.*, 2018) attempted to combine spline modelling (e.g. loess) with sparse Principal Component Analysis to explore the link between chemistry and microbial community data in the biodegradation of chemically dispersed oil, but their approach was not specifically looking for multi-omics signatures.

We propose a computational approach to integrate microbiome data with multi-omics datasets in longitudinal studies. Our approach includes smoothing splines in a linear mixed model framework to model profiles across groups of samples, and builds on the ability of sparse multivariate ordination methods to identify correlated sets of variables across the data types, and across time. Our framework encompasses data pre-processing, modelling, data clustering and integration. It is highly flexible in handling one or several longitudinal studies with a small number of time points, to identify groups of taxa with similar behaviour over time, and posit novel hypothesis about symbiotic relationships, interactions or competitions in a given condition or environment, as we illustrate in two case studies.

2 Method

Our proposed approach includes pre-processing for microbiome data, spline modelisation within a linear mixed model framework, and a multivariate analysis for clustering and data integration (Figure 1).

2.1 Pre-processing of microbiome data

We assume the data are in raw count formats resulting from bioinformatics pipelines such as QIIME (Caporaso *et al.*, 2010) or FROGS (Escudié *et al.*, 2017) for 16S amplicon data. Here we consider the OTU taxonomy level, but other levels can be considered, as well as other types of microbiome-derived data, such as whole genome shotgun sequencing. The data processing step is described in Lê Cao *et al.* (2016a) and consists of:
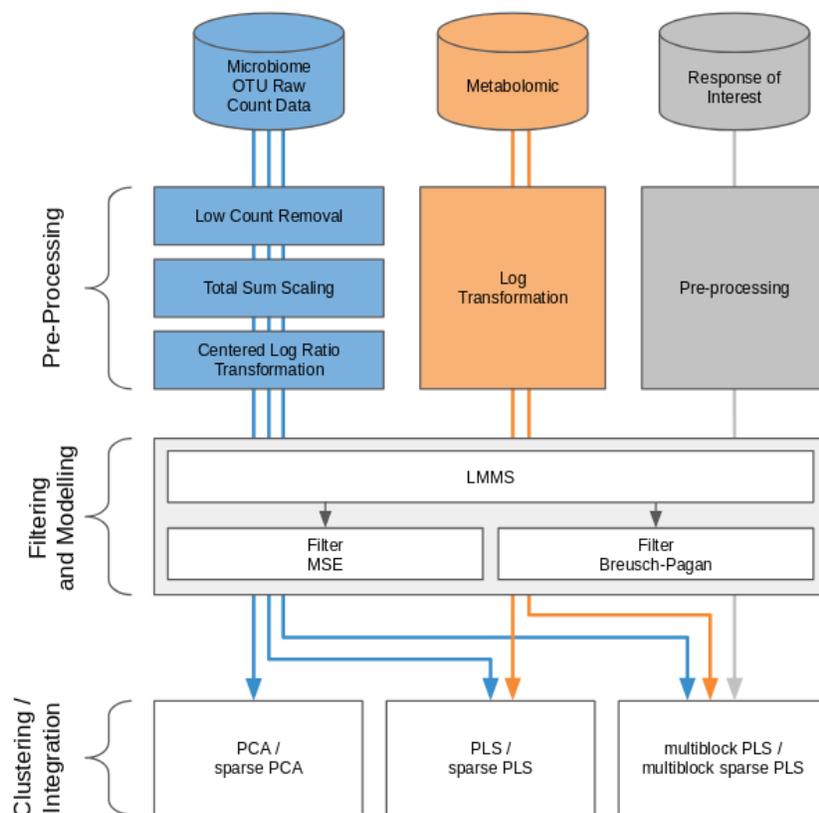
Figure 1: Workflow diagram for longitudinal integration of microbiota studies. We consider studies for the analysis of the microbiota through OTU (16S amplicon) or gene (whole genome shotgun) counts. This information can be complemented by additional information at the microbiota level, such as metabolic pathways measured with metabolomics, or information measured at a macroscopic level resulting from the aggregated actions of the microbiota.

1. Low Count Removal: Only OTUs whose proportional counts exceeded 0.01% in at least one sample were considered for analysis. This step aims to counteract sequencing errors (Kunin *et al.*, 2010).

2. Total Sum Scaling (TSS) can be considered as a 'normalisation' process to account for uneven sequencing depth across samples. TSS divides each OTU count by the total number of counts in each individual sample but generates compositional data expressed as proportions.

3. Centered Log Ratio transformation addresses in a practical way the compositionality issue, by projecting the data into a Euclidean space (Aitchison, 1982; Fernandes *et al.*, 2014; Gloor *et al.*, 2017).

2.2 Time profile modelling

2.2.1 Linear Mixed Model splines (LMMS)

The LMMS modelling approach proposed by Straube *et al.* (2015) takes into account between and within individual variability and irregular time sampling. LMMS is based on a linear mixed model representation of penalised splines (Durbán *et al.*, 2005) for different types of models. Through this flexible approach of serial fitting, LMMS avoids under- or over-smoothing. Briefly, four types of models are consecutively fitted in our framework on the TSS-CLR data:

(1) A simple linear regression of taxa abundance on time, estimated via ordinary linear least squares - a straight line that assumes the response is not affected by individual variation.

3

(2) A penalised spline proposed by Durbán *et al.* (2005) to model nonlinear response patterns.

(3) A model that accounts for individual variation with the addition of a subject-specific random effect to the mean response in model (2).

(4) An extension to model (3) that assumes individual deviations are straight lines, where individual-specific random intercepts and slopes are fitted.

All four models are described in Appendix A. Straube *et al.* 2015 showed that the proportion of profiles fitted with the different models increased in complexity with the organism considered. Different types of splines can be considered in models (2) - (4), including a cubic spline basis (Verbyla *et al.*, 1999), a penalised spline and a cubic penalised spline. A cubic spline basis uses all inner time points of the measured time interval as knots, and is appropriate when the number of time points is small (≤ 5), whereas the penalised spline and cubic penalised spline bases use the quantiles of the measured time interval as knots, see Ruppert (2002). In our case studies, we used penalised splines. The LMMS models are implemented in the R package `lmms` (Straube *et al.*, 2016).

2.2.2 Prediction and interpolation

The fitted splines enable us to predict or interpolate time points that might be missing within the time interval (e.g. inconsistent time points between different types of data or covariates). Additionally, interpolation is useful in our multivariate analyses described below to smooth profiles, and when the number of time points is small (≤ 5). In the following section, we therefore consider data matrices X ($T \times P$), where T is the number of (interpolated) time points and P the number of taxa. The individual dimension has thus been summarised through the spline fitting procedure, so that our original data matrix of size ($N \times P \times T$), where N is the number of biological samples, is now of size ($T \times P$).

2.3 Filtering profiles after modelling

A simple linear regression model (1) might be the result of highly noisy data. To retain only the most meaningful profiles, the quality of these models was assessed with a Breusch-Pagan test to indicate whether the homoscedasticity assumption of each linear model was met (Breusch and Pagan, 1979) . We also used a threshold based on the mean squared error (MSE) of the linear models, by only including profiles for which their MSE was below the maximum MSE of the more complex fitted models (1) - (4). The latter filter was only applied when a large number of linear models (1) were fitted and the Breusch-Pagan test was not considered stringent enough.

2.4 Clustering time profiles

2.4.1 PCA and sparse PCA

Multivariate dimension reduction techniques such as Principal Component Analysis (PCA, Jolliffe 2005) and sparse PCA (Huang and Zheng, 2006) can be used to cluster taxa profiles. To do so, we consider as data input the X ($T \times P$) spline fitted matrix. Let $t_1, t_2, \ldots, t_H$ denote the H principal components of length T and their associated $v_1, v_2, \ldots, v_H$ factors - or loading vectors, of length P. For a given PCA dimension h, we can extract a set of strongly correlated profiles by considering taxa with the top absolute coefficients in v_h. Those profiles are linearly combined to define each component t_h, and thus, explain similar information on a given component. Different clusters are therefore obtained on each dimension h of PCA, $h = 1 \ldots H$. Each cluster h is then further separated into two sets of profiles which we denote as 'positive' or 'negative' based on their correlation (see Figure 3).

A more formal approach can be used with sparse PCA. Sparse PCA includes ℓ_1 penalisations on the loading vectors to select variables that are key for defining each component, and are highly correlated within a component (see Huang and Zheng 2006 for more details).

2.4.2 Choice of the number of clusters in PCA

We propose to use the average silhouette coefficient (Rousseeuw, 1987) to determine the optimal number of clusters, or dimensions H, in PCA. For a given identified cluster and observation i, the silhouette

4

coefficient of i is defined as

$$s(i) = \frac{b(i) - a(i)}{\max(a(i), b(i))} \tag{5}$$

where $a(i)$ is the average distance between observation i and all other observations within the same cluster, and $b(i)$ is the average distance between observation i and all other observations in the nearest cluster. A silhouette score is obtained for each observation and averaged across all silhouette coefficients, ranging from -1 (poor) to 1 (good clustering).

We adapted the silhouette coefficient to choose the number of components or clusters in PCA and sPCA (i.e. $2 \times H$ clusters), as well as the number of profiles to select for each cluster. Each observation in Eq. (5) now represents a fitted LMMS profile, and the distance between two profiles is calculated using the Spearman Correlation coefficient.

Within a given cluster, we calculate the silhouette coefficient of each LMMS profile and apply the following empirical rules for cluster assignation: a coefficient > 0.5 assigns the profile to the cluster, a value between 0 and 0.5 indicates an uncertain assignment as the profile can be assigned to one or two clusters, while a negative value indicates that the profile should not be assigned to this particular cluster.

To choose the appropriate number of profiles per sPCA component, we perform as follows: For each component, we set a grid of number of profiles to be retained with sPCA and calculated the average silhouette coefficient per cluster (there are two clusters per component). The final number of profiles to select is arbitrarily set when we observe a sudden decrease in the average silhouette coefficient (see Figure 4).

We also used the average silhouette coefficient to assess the quality of different clustering approaches, as illustrated in the Results Section: a greater average silhouette coefficient indicates a better clustering of the profiles.

2.5 Integration

2.5.1 Multiblock PLS methods

To integrate multiple datasets (also called *blocks*) measured on the same biological samples we used multivariate methods based on Projection to Latent Structures (PLS) methods (Wold, 1975), which we broadly term *multiblock PLS* approaches. For example, we can consider Generalised Canonical Correlation Analysis (GCCA, Tenenhaus and Tenenhaus 2011; Tenenhaus *et al.* 2014), which, contrary to what its name suggests, generalises PLS for the integration of more than two datasets. Recently, we have developed the DIABLO method to discriminate different phenotypic groups in a supervised framework (Singh *et al.*, 2019). In the context of this study however, we present the sparse GCCA in an unsupervised framework, where input datasets are spline-fitted matrices.

We denote Q data sets $X^{(1)}(T \times P_1)$, $X^{(2)}(T \times P_2)$, ..., $X^{(Q)}(T \times P_Q)$ measuring the expression levels of P_q variables of different types (taxa, 'omics, continuous response of interest), modelled on T (interpolated) time points, $q = 1, \ldots, Q$. GCCA solves for each component $h = 1, \ldots, H$:

$$\max_{a_h^{(1)}, \ldots, a_h^{(Q)}} \sum_{q,j=1, q \neq j}^{Q} c_{q,j} \, \mathrm{cov}(X_h^{(q)} a_h^{(q)}, X_h^{(j)} a_h^{(j)}), \qquad \text{s.t.} \quad ||a_h^{(q)}||_2 = 1 \text{ and } ||a_h^{(q)}||_1 \leq \lambda^{(q)} \tag{6}$$

where $\lambda^{(q)}$ is the ℓ_1 penalisation parameter, $a_h^{(q)}$ is the loading vector on component h associated with the residual (deflated) matrix $X_h^{(q)}$ of the data set $X^{(q)}$, and $C = \{c_{q,j}\}_{q,j}$ is the design matrix. C is a $Q \times Q$ matrix that specifies whether datasets should be correlated and includes values between zero (datasets are not connected) and one (datasets are fully connected). Thus, we can choose to take into account specific pairwise covariances by setting the design matrix (see Rohart *et al.* 2017 for implementation and usage) and model a particular association between pairs of datasets, as expected from prior biological knowledge or experimental design. In our integrative case study, we used sparse PLS, a special case of Eq. (6) to integrate microbiome and metabolomic data, as well as sparse multiblock PLS to also integrate variables of interest. Both methods were used with a fully connected design.

The multiblock sparse PLS method was implemented in the `mixOmics` R package where the ℓ_1 penalisation parameter is replaced by the number of variables to select, using a soft-thresholding approach (see more details in Rohart *et al.* 2017).

2.5.2 Parameters tuning

The integrative methods require choosing the number of components H, defined as $t_h^{(q)} = a_h^{(q)} X_h^{(q)}$ with the notations from Section 2.5.1, and number of profiles to select on each PLS component and in each dataset. We generalised the approach described in Section 2.4.2 using the silhouette coefficient based on a grid of parameters for each dataset and each component.

2.6 Case studies

2.6.1 Infant gut microbiota development

The gastrointestinal microbiome of 14 babies during the first year of life was studied by Palmer *et al.* (2007). The authors collected an average of 26 stool samples from healthy full-term infants. As infants quickly reach an adult-like microbiota composition, we focused our analyses on the first 100 days of life. Infants who received an antibiotic treatment during that period were removed from the analysis, as antibiotics can drastically alter microbiome composition (Dudek-Wicher *et al.*, 2018).

The dataset we analysed included 21 time points on average for 11 selected infants (Figure 2). Samples were collected daily during days 0-14 and weekly after the second week. We separated our analyses based on the delivery mode (C-section or vaginal), as this is known to have a strong impact on gut microbiota colonisation patterns and diversity in early life (Rutayisire *et al.* (2016)).
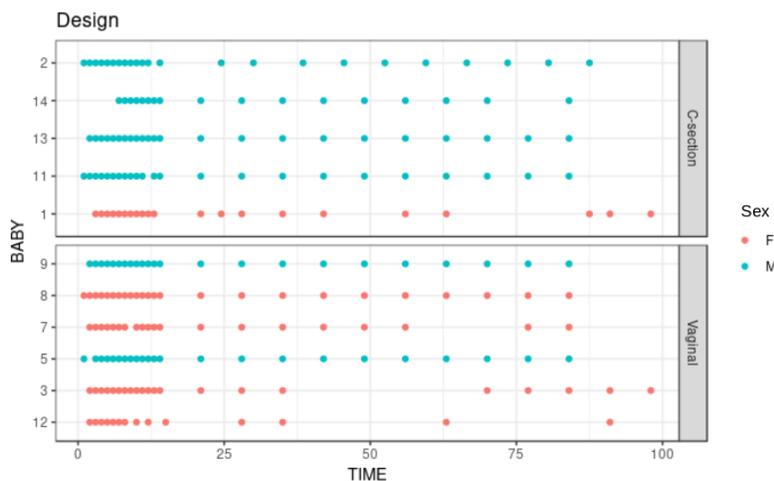

Figure 2: Infant gut microbiota development study: stool samples were collected from six male and five female babies over the course of 100 days. Samples were collected daily during days 0-14 and weekly thereon until day 100. Time is indicated on the x-axis in days. As delivery method is known to be a strong influence on gut microbiome colonisation, the data are separated according to either C-section or vaginal birth.

2.6.2 Waste degradation study

Anaerobic digestion (AD) is a highly relevant microbial process to convert waste into valuable biogas. It involves a complex microbiome that is responsible for the progressive degradation of molecules into methane and carbon dioxide. In this study, AD's biowaste was monitored across time (more than 150 days) in three lab-scale bioreactors as described in (Poirier *et al.*, 2016). The purpose of the study was to investigate the

6

relationship between biowaste degradation performance, microbial dynamics and metabolomic dynamics across time.

We focused our analysis on days 9 to 57, that correspond to the most intense biogas production. Degradation performance was monitored through 4 parameters: methane and carbon dioxide production (16 time points) and accumulation of acetic and propionic acid in the bioreactors (5 time points). Microbial dynamics were profiled with 16S RNA gene metabarcoding as described in Poirier *et al.* (2016) and included 4 time points and 90 OTUs. A metabolomic assay was conducted on the same biological samples on 4 time points with gas chromatography coupled to mass spectrometry GC-MS after solid phase extraction to monitor substrates degradation (Limam *et al.*, 2010). The `XCMS` R package (version 1.52.0) was used to process the raw metabolomics data (Smith *et al.*, 2006). GC-MS analyses focused on 20 peaks of interest identified by the National Institute of Standards and Technology database. Data were then log-transformed for statistical analysis.

3   Results

3.1   Clustering time profiles: Infant gut microbiota development study

3.1.1   Pre-processing and modelling

A total of 2,149 taxa were identified in the raw data (Table 1). After the pre-processing steps illustrated in Figure 1, a smaller number of OTUs were found in faecal samples of babies born by C-section than vaginal delivery. Similarly, a simple linear regression model showed a smaller proportion of OTUs in babies born via C-section (73%) than vaginal delivery (81%), and this was also observed after the filtering step (Table 1).

3.1.2   Comparison of PCA and functional PCA

Functional Principal Component Analysis (fPCA) was proposed by Ramsay and Silverman (2005) and is a popular approach to cluster longitudinal data (Jacques and Preda, 2014). fPCA extracts 'modes of variation' and performs functional clustering and identification of longitudinal data sub-structures using k-centres functional Clustering (k-CFC, Chiou and Li 2007 or model-based clustering using an Expectation-Maximization algorithm (Chen *et al.*, 2012). Both clustering methods are implemented in `fdapace` R package (Dai *et al.*, 2018).

Based on the silhouette coefficient, we included 4 clusters (i.e. two components) in PCA, and set the same number of clusters in fPCA for comparative purposes. PCA clustering outperformed fPCA for each delivery mode dataset that was analysed (see Table 2). The resulting fPCA clustering is displayed in Figure 4 for babies born via vaginal delivery. We found that the EM approach in fPCA tended to cluster a larger number of uncorrelated OTUs compared to the k-CFC approach (average silhouette coefficient = 0.07 for EM and 0.61 for k-CFC).

3.1.3   Clusters of profiles

We used sPCA to select key OTU profiles for each cluster. This step is essential for discarding profiles that are distant from the average cluster profile and thus not informative. As expected, we observed an overall increase in the silhouette average coefficient for the sPCA clustering compared to PCA, indicating a better clustering capability (see Table 2). According to the silhouette average coefficient, vaginal delivery showed the best partitioning for PCA clustering (0.87, Table 2). Cluster 1 (denoted 'component 1 positive' in Figure 3 **A**) showed an increase in the abundance profile of species, including some that are characteristic of a healthy "adult-like" gut microbiome composition such as the clade *Bacteroidetes* (Thursby and Juge, 2017). In cluster 2 ('component 1 negative'), profile abundance tended to decrease and corresponded to genera found in abundance in vaginal and skin microbiota, such as *Lactobacillus* and *Propionibacterium* (Grice and Segre, 2011; Bing *et al.*, 2012). Clusters 3 and 4 (denoted 'component 2 positive and negative') highlighted taxa with negatively correlated profiles. Thus, with this preliminary PCA analysis, we were able to rebuild a partial history behind the development of the gut microbiota. Vaginal species that initially colonized in the gut progressively disappeared to enable species that characterize adult gut
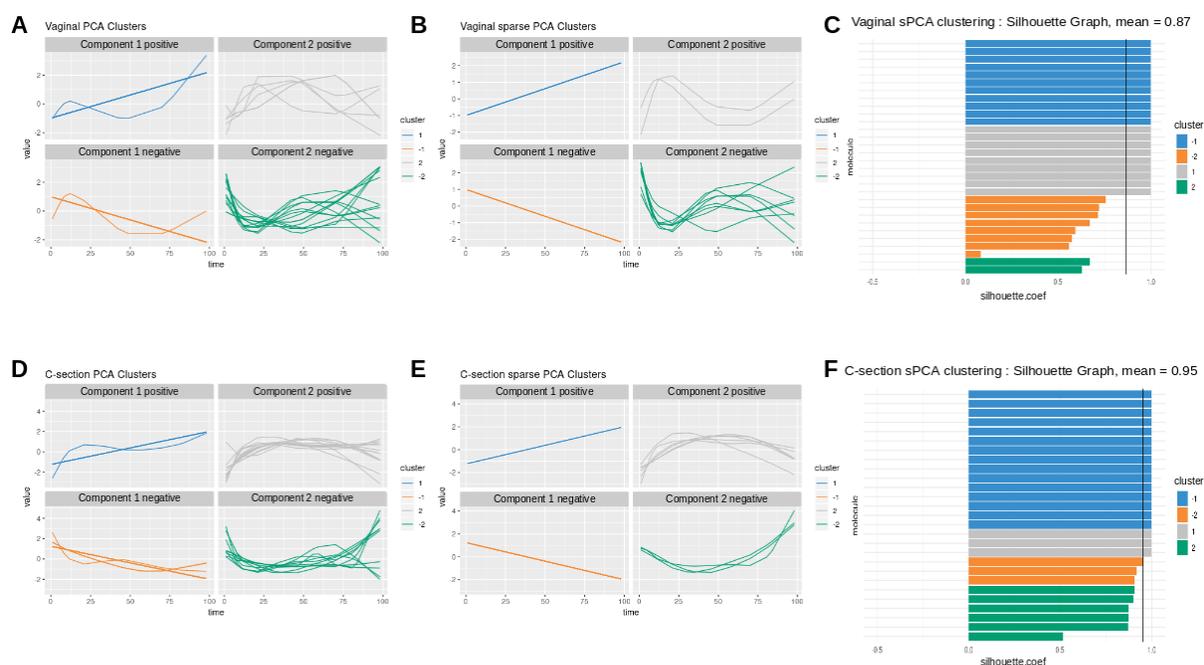
Figure 3: Vaginal (first row) and C-section delivery babies (second row). (**A**) - (**B**), (**D**) - (**E**): OTU profiles clustered with either PCA or sPCA. Each line represents the abundance of a selected OTU across time. OTUs were clustered according to their contribution on each component for PCA, and ℓ_1 penalisation for sPCA. The PCA clusters were further separated into profiles with a positive or negative correlation. Profiles were scaled to improve visualisation. (**C**) - (**F**): Silhouette profile for each identified clustering. Each bar represents the silhouette coefficient of a particular OTU and colors represent assigned clusters. The average coefficient is represented by a vertical black line. A greater average silhouette coefficient means a better partitioning state. (**C**): vaginal delivery babies with sPCA (average silhouette coefficient = 0.87); (**F**): C-section delivery babies with sPCA (average silhouette coefficient = 0.95).

microbiota.

For babies born by C-section, 4 clusters were identified by PCA (Fig. 3 **D**). Clusters 1 and 2 ('component 1 positive and negative') displayed a clear increase and decrease respectively in abundance profile. However none of the cluster 2 species are known to characterize, or were found in, vaginal delivery, suggesting that the infant gut was first colonized by the operating room microbes as already demonstrated by Shin *et al.* (2015). Cluster 3 ('component 2 positive') revealed transitory states of increase then decrease of abundance profiles, while cluster 4 ('component 2 negative') showed a decrease then an increase.

3.2 Clustering omics: waste degradation study

3.2.1 Pre-processing and modelling

A total of ninety OTUs were identified in the 12 samples of the initial dataset (Table 4). After pre-processing, 51 OTUs were retained. Approximately 60% (resp. 50%) of the OTUs (resp. metabolites) were fitted with linear regression models (1) and 40% (resp. 50%) were modelled by more complex splines models (2) - (4). All performance measures were also modelled by splines. During the filtering step, 7 OTUs and 4 metabolites that were fitted with linear regression models were discarded.

3.2.2 sPCA on concatenated datasets

As a first and naive attempt to jointly analyse microbial, metabolomic and performance measures, all three datasets were concatenated then analysed with sPCA. Only a very small number of profiles from the
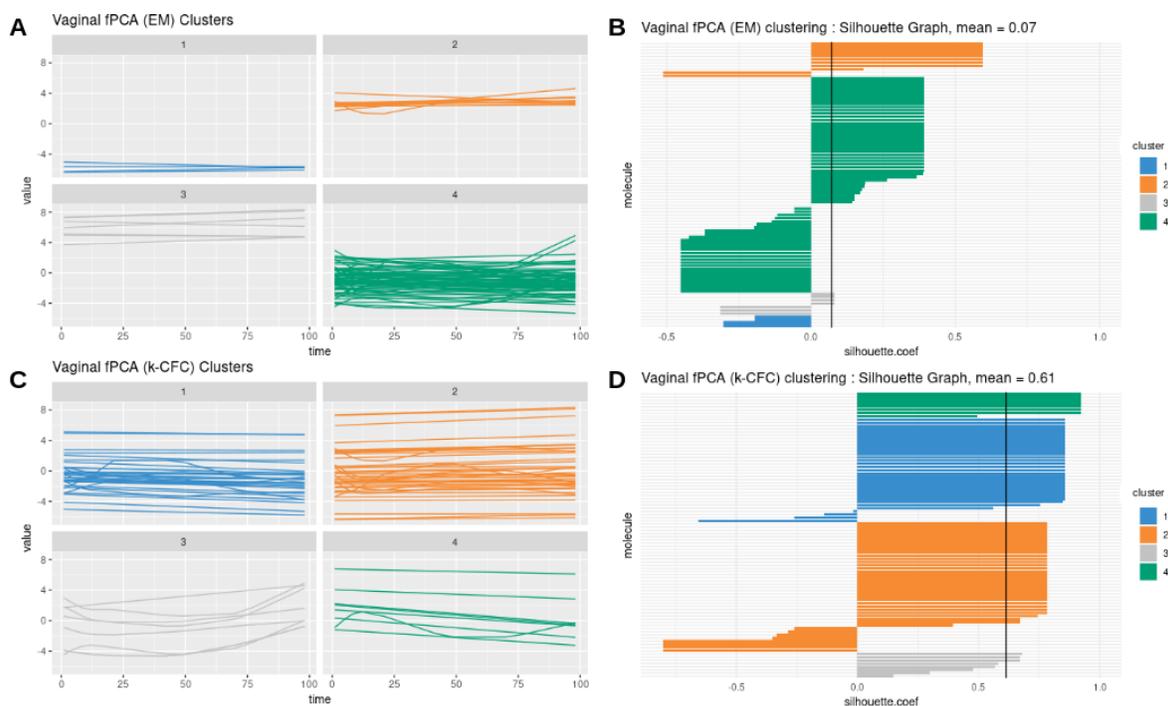
Figure 4: fPCA Expectation-Maximization clustering (first row) and k- Center Functional Clustering (second row). (**A**) - (**C**): Vaginal OTU profiles clustered with either EM or k-CFC. Each line represents the abundance of a selected OTU across time. (**B**) - (**D**): Silhouette coefficient for each profile and each clustering. Each bar represents the silhouette coefficient of a particular OTU and colors represent assigned clusters. The average coefficient is represented by a vertical black line. The average silhouette coefficient was 0.07 for EM clustering and 0.61 for k-CFC clustering.

different datasets were selected. This small selection is likely due to the high variability in each data type. Selected variables included mainly OTUs and performance measures. These were assigned to four clusters and included respectively 1, 3, 2 and 3 OTUs with 0, 1, 2 and 0 metabolites and 2, 0, 1 and 0 performance measures. The average silhouette coefficient was 0.744, a potentially sub-optimal clustering compared to our analyses presented in the next Section. This preliminary investigation highlighted the limitation of sPCA to identify a sufficient number of correlated profiles from disparate sources.

3.2.3 Microbiome - metabolomic integration with sPLS

The results from the sPLS analysis are shown in Figure 5. Four clusters of variables were selected. The first cluster (denoted 'component 1 negative') included 10 OTUs and 4 metabolite variables, and showed increasing abundance until a plateau was reached at approximately 40 days. The OTUs were microorganisms often recovered during anaerobic digestion of biowaste, such as methanogenic archaea of *Methanosarcina* genus or bacteria of *Clostridiales*, *Acholeplasmatales*, and *Anaerolineales* orders (Poirier *et al.*, 2016). Their abundance increased while biowaste was degraded, until there was no more biowaste available in the bioreactor. Their abundance was correlated to the intensity of various metabolites produced during the AD process, such as benzoic acid that is formed during the degradation of phenolic compounds (Hoyos-Hernandez *et al.*, 2014), or phytanic acid, known to be produced during the fermentation of plant materials in the ruminant gut (Watkins *et al.*, 2010), as well as indole-2-carboxylic acid. Cluster 2 (component 1 positive) included 10 OTUs and 4 metabolites. These profiles were negatively correlated to Cluster 1, and their abundance decreased with time. OTUs mainly belonged to the *Bacteroidales* order. They were present in the initial inoculum but did not survive in this experiment, as the operating conditions or the substrate were not optimal for their growth, as observed in other studies (Madigou *et al.*, 2019). Metabolites identified in Cluster 2 were present in the biowaste and were degraded during the

9

experiment. They included fatty acids (decanoic and tetradecanoic acids) that can be found in oil, or 3-(3-Hydroxyphenyl)propionic acid, arising from digestion of aromatic amino-acids or breakdown product of lignin or other plant-derived phenylpropanoids. As their profile was negatively correlated to those from cluster 1, it is likely that these metabolites were consumed by OTUs assigned to cluster 1 (Torres *et al.*, 2003). Cluster 3 (component 2 negative) included 1 OTU and 5 metabolites. Profiles decreased slowly with time. One OTU of *Clostridiales* order appears to have been out-competed by other OTUs or phase active only during the first days of the degradation. Among the metabolites of this cluster, Hydrocinnamic and 3,4-Dihydroxyhydrocinnamic acids are commonly found in plant biomass and its residues (Boerjan *et al.*, 2003). Their molecular structure may have contributed to their slower degradation compared to other molecules. Finally, Cluster 4 (component 2 positive) included 11 OTUs and 3 metabolites with slow abundance increase. OTUs of this group were very varied with 8 orders represented. They may have slower growth rates than OTUs of cluster 1 or were involved in the last steps of the degradation. Metabolites included N-Acetylanthranilic acid and Dehydroabietic acid that were likely produced by microorganisms and accumulated during the anaerobic digestion process. The average silhouette coefficient was 0.954 and confirmed that sPLS led to better clustering of the different types of profiles than sPCA in Section 3.2.2.
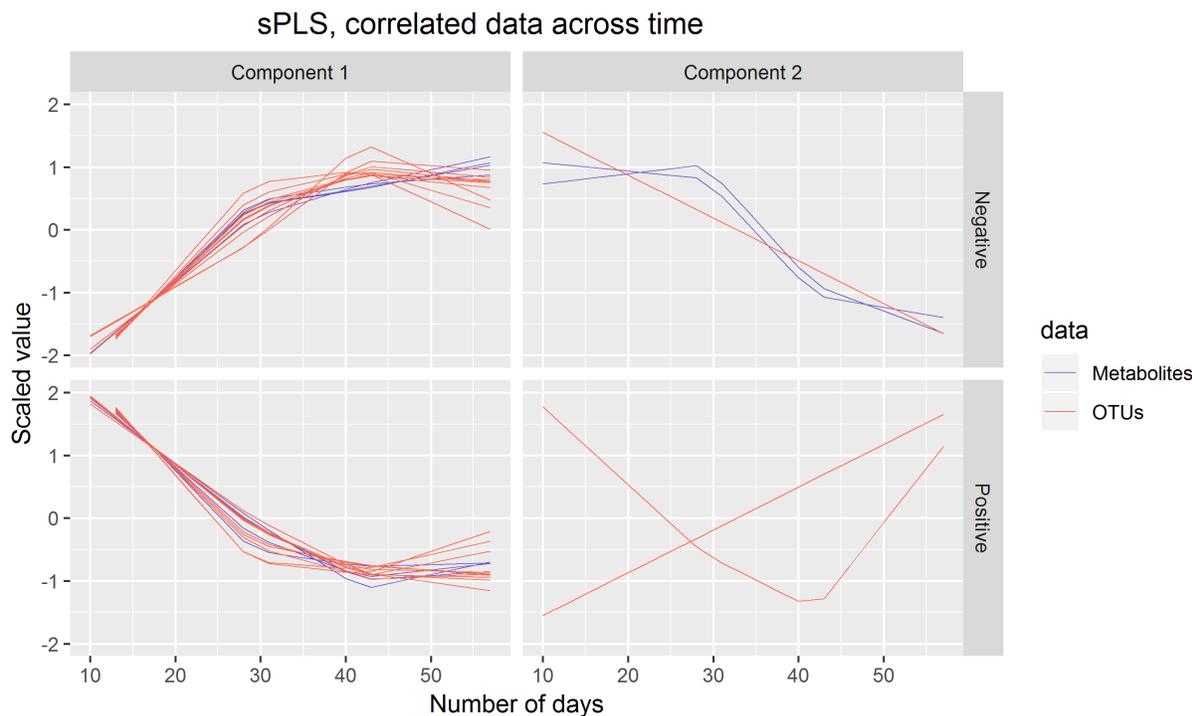

Figure 5: Biowaste study: sPLS analysis identified correlated profiles of OTUs and metabolites. Each line represents the abundance of selected OTUs and metabolites across time. OTUs and metabolites were clustered according to their contribution on each component for sPLS. The clusters were further separated into profiles with a positive or negative correlation.

3.2.4 Microbiome, metabolomic and performance data integration with block sPLS

Figure 6 illustrates the results from the integration of the three datasets, where the performance data are considered as the response of interest. Similar to the sPLS analysis, block sPLS assigned profiles to four clusters, with an average silhouette coefficient of 0.909. Two performance variables (methane and carbon dioxyde production) were assigned to cluster 1. This result is biologically relevant, as biogas is the final output of the AD reaction and is known to be associated with microbial activity and growth. Moreover, it is produced by archaea, such as *Methanosarcina*, also selected in this cluster. In Cluster 2 (component 2 negative), we identified acetate produced by bacteria in the early days of the incubation and consumed by archaea (Cluster 1) to produce biogas. Propionate was assigned to the third cluster, as its degradation

only starts when all acetate is degraded (Chapleur *et al.*, 2014). Cluster 4 was composed of only OTUs and metabolites and was similar to the one obtained with sPLS.
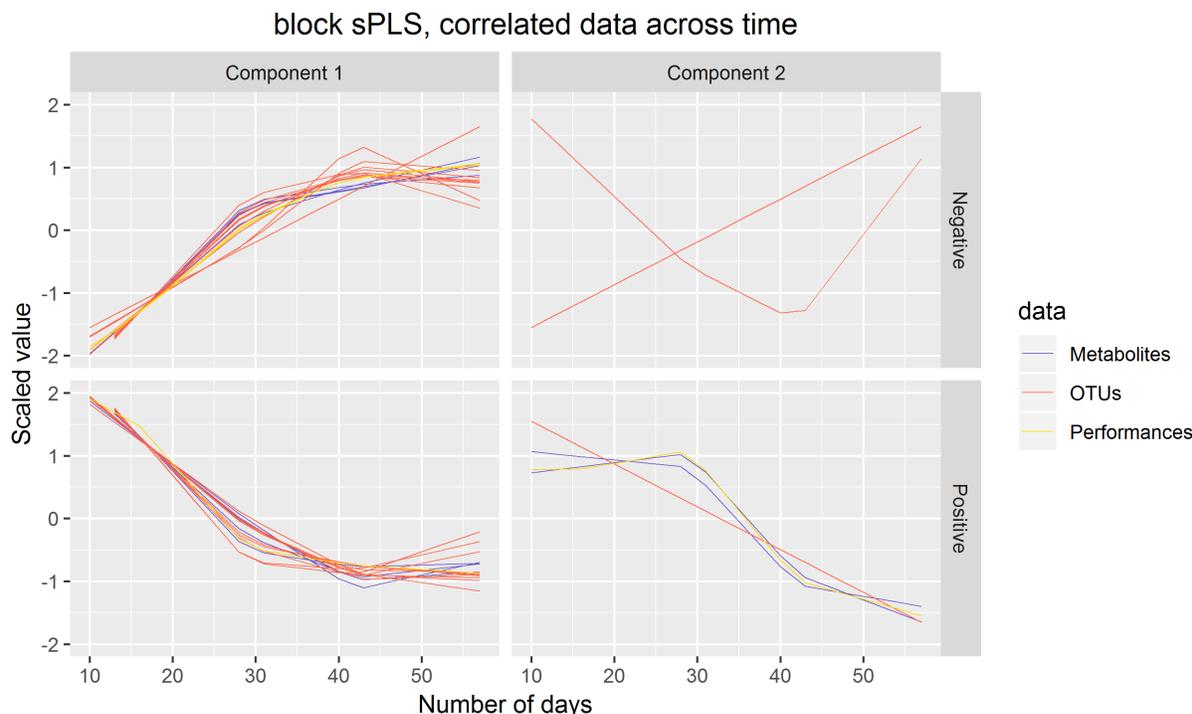

Figure 6: Biowaste degradation study: integration of OTUs, metabolites and performance measures with block sPLS. Each line represents the abundance of selected OTUs, metabolites and performance measures across time. OTUs, metabolites and performance measures were clustered according to their contribution on each component for block sPLS. The clusters were further separated into profiles with a positive or negative correlation.

4   Discussion

Advances in technology and reduced sequencing costs have resulted in the emergence of new and more complex experimental designs that combine multiple omic datasets and several sampling times from the same biological material. Thus, the challenge is to integrate longitudinal, multi-omic data to capture the complex interactions between these omic layers and obtain a holistic view of biological systems. In order to integrate longitudinal data from microbial communities with other omics, meta-omics or other clinical variables, we proposed a data-driven analytical framework to identify highly correlated temporal profiles between these multiple and heterogeneous datasets.

In the proposed framework, the microbial counts of the microbiota's constituent species are normalised for uneven sequencing library sizes and compositional data. Modelling with linear mixed model splines enables us to reduce the dimension of the data across the different biological replicates and take into account the individual variability due to either technical or biological sources. This approach also enables us to compare data analysed at different time points (e.g bioreactor study). Lastly, we clustered the data using multivariate dimension reduction techniques on the spline models that further allowed integration between different data types, and the identification of the main patterns of longitudinal variation.

A similar approach to ours was proposed by Ribicic *et al.* (2018) who used linear regression models coupled with multivariate dimension reduction methods on 16S and chemical longitudinal data to study the effects of oil temperature and composition on the biodegradation of chemically dispersed oil. We have

11

taken their approach one step further, with the appropriate handling of compositional data, a fully developed modelling framework, and the identification of key profiles assigned to different clusters using sparse multivariate integrative methods.

Integrating different types of microbiome longitudinal data (abundance, activity, metabolic pathways, macroscopic output...) can be naively performed by concatenating all datasets. However, we showed that this approach was unsuccessful at selecting a sufficiently large number of profiles of different types, and thus does not shed light on the holistic view of the ecosystem dynamics (bioreactor study). Our integrative multivariate methods sPLS and block sPLS are better suited for the integration task, as they do not merge but rather statistically correlate components built on each dataset, and avoid unbalance in the signature when one dataset might be either more informative, less noisy, or larger than the other datasets.

When compared with fPCA, that uses either k-CFC or EM clustering algorithms, we showed that our approach led to better clustering performance. In addition, the sparse multivariate approaches sPCA and block sPLS enable the identification of key profiles to improve biological interpretation. Note however that fPCA might be better suited than our approach for a large number of time points, as we discuss next.

We have identified several limitations in our proposed framework. Firstly, a high individual variability between biological replicates limits the LMMS modelling step, resulting in simple linear regression models to fit the data. Whilst a straight line model may accurately describe temporal dynamics, it could also be due to a poor quality of fit. We have implemented the Breusch-Pagan test to address this issue. Alternatively, in the case of a very high inter-individual variability that prevents appropriate smoothing, one could consider *N of One* analyses as proposed by Gerber *et al.* (2012); Äijö *et al.* (2017) with time dynamical probabilistic models. Secondly, a large number of time points can result in the modelling of noisy profiles and clusters, often due to high individual variability. Highly variable and vastly different profiles can also be difficult to cluster appropriately. Therefore, this framework is recommended when the number of time points remains small (5-10) and when regular and similar trends are expected from the data. Thirdly, our framework does not include time delay analysis, even though dynamic delays between different types of molecules (e.g. DNA, RNA, metabolites...) can be expected. For example, 16S data describes the abundance of the microorganisms while metabolites are the consequences of their activity, and performances are the macroscopic resulting output. Potential delays between these molecules can be detected using other techniques, such as the Fast Fourier Transform approach from Straube *et al.* (2017) and will be further investigated in our future work.

To summarise, we have proposed one of the first computational framework to integrate longitudinal microbiome data with other omics data or other variables generated on the same biological samples or material. The identification of highly-correlated key omics features can help generate novel hypotheses to better understand the dynamics of biological and biosystem interactions. Thus, our data-driven approach will open new avenues for the exploration and analyses of multi-omics studies.

Conflict of Interest Statement

The authors declare that the research was conducted in the absence of any commercial or financial relationships that could be construed as a potential conflict of interest.

Author Contributions

All authors contributed to the design of the study; AB and OC performed the statistical analyses; AB, OC and KALC wrote the manuscript. All authors contributed to manuscript revision, read and approved the submitted version.

Funding

Supplemental Data

Data Availability Statement

Infant gut microbiota phylochip raw data can be found in Palmer *et al.* (2007). The microbiome and
performance datasets for the bioreactor study can be found in Poirier and Chapleur (2018), metabolomic
data is available on request. In-house scripts and code to conduct both case study analysis, are available
in a Github public repository : https://github.com/abodein/timeOmics

Table 1: Number of OTUs identified, and linear model types fitted according to delivery mode.

		C-section	Vaginal
Identified OTUs		2,149	2,149
# OTUs after pre-processing		107	117
Linear model types	(1)	78	95
	(2)	29	22
Linear model types after filtering	1	42	68
	2	29	22

Table 2: Average silhouette coefficient according to clustering method

	PCA	sPCA	fPCA (k-CFC)	fPCA(EM)
Vaginal	0.84	0.95	0.61	0.07
C-section	0.87	0.86	0.69	0.35

Table 3: Number of OTUs per cluster identified with PCA clustering and OTUs selected in brackets with
sparce PCA.

	C-section	Vaginal
Cluster 1 (comp 1 positive)	11 (3)	32 (9)
Cluster 2 (comp 1 negative)	35 (15)	38 (11)
Cluster 3 (comp 2 positive)	15 (6)	6 (2)
Cluster 4 (comp 2 negative)	10 (3)	14 (8)

References

Äijö, T., Müller, C. L., and Bonneau, R. (2017). Temporal probabilistic modeling of bacterial compositions derived from 16s rrna sequencing. *Bioinformatics*, **34**(3), 372–380.

Aitchison, J. (1982). The statistical analysis of compositional data. *Journal of the Royal Statistical Society. Series B (Methodological)*, pages 139–177.

Baksi, K. D., Kuntal, B. K., and Mande, S. S. (2018). 'time': A web application for obtaining insights into microbial ecology using longitudinal microbiome data. *Frontiers in Microbiology*, **9**, 36.

Bing, M., Forney, L., and Ravel, J. (2012). The vaginal microbiome: rethinking health and diseases. *Annu Rev Microbiol*, **66**, 371–89.

Boerjan, W., Ralph, J., and Baucher, M. (2003). Lignin biosynthesis. *Annual review of plant biology*, **54**(1), 519–546.

Table 4: OTUs, metabolites and performance modelling and filtering in the bioreactor study. Only OTUs data were preprocessed.

Type of features		OTUs	Metabolites	Performance
Number of features		90	20	4
# features after pre-processing		51	NA	NA
Linear model types	(1)	30	10	0
	(2)	19	0	2
	(3)	2	4	0
	(4)	0	6	2
Linear model types after filtering	(1)	24	6	0
	(2)	19	0	2
	(3)	2	4	0
	(4)	0	6	2

Breusch, T. S. and Pagan, A. R. (1979). A simple test for heteroscedasticity and random coefficient variation. *Econometrica: Journal of the Econometric Society*, pages 1287–1294.

Bucci, V., Tzen, B., Li, N., Simmons, M., Tanoue, T., Bogart, E., Deng, L., Yeliseyev, V., Delaney, M. L., Liu, Q., *et al.* (2016). Mdsine: Microbial dynamical systems inference engine for microbiome time-series analyses. *Genome biology*, **17**(1), 121.

Caporaso, J. G., Kuczynski, J., Stombaugh, J., Bittinger, K., Bushman, F. D., Costello, E. K., Fierer, N., Pena, A. G., Goodrich, J. K., Gordon, J. I., *et al.* (2010). Qiime allows analysis of high-throughput community sequencing data. *Nature methods*, **7**(5), 335.

Chapleur, O., Bize, A., Serain, T., Mazéas, L., and Bouchez, T. (2014). Co-inoculating ruminal content neither provides active hydrolytic microbes nor improves methanization of 13c-cellulose in batch digesters. *FEMS microbiology ecology*, **87**(3), 616–629.

Chen, W., Maitra, R., and Melnykov, V. (2012). *EMCluster: EM Algorithm for Model-Based Clustering of Finite Mixture Gaussian Distribution*.

Chiou, J.-M. and Li, P.-L. (2007). Functional clustering and identifying substructures of longitudinal data. *Journal of the Royal Statistical Society: Series B (Statistical Methodology)*, **69**(4), 679–699.

Clemmensen, L., Hastie, T., Witten, D., and Ersbøll, B. (2011). Sparse discriminant analysis. *Technometrics*, **53**(4), 406–413.

Dai, X., Hadjipantelis, P. Z., Han, K., and Ji, H. (2018). *fdapace: Functional Data Analysis and Empirical Dynamics*. R package version 0.4.0.

Dudek-Wicher, R. K., Junka, A., and Bartoszewicz, M. (2018). The influence of antibiotics and dietary components on gut microbiota. *Przeglad gastroenterologiczny*, **13**(2), 85.

Durbán, M., Harezlak, J., Wand, M., and Carroll, R. (2005). Simple fitting of subject-specific curves for longitudinal data. *Statistics in medicine*, **24**(8), 1153–1167.

Escudié, F., Auer, L., Bernard, M., Mariadassou, M., Cauquil, L., Vidal, K., Maman, S., Hernandez-Raquet, G., Combes, S., and Pascal, G. (2017). Frogs: find, rapidly, otus with galaxy solution. *Bioinformatics*, **34**(8), 1287–1294.

Faust, K., Lahti, L., Gonze, D., De Vos, W. M., and Raes, J. (2015). Metagenomics meets time series analysis: unraveling microbial community dynamics. *Current opinion in microbiology*, **25**, 56–66.

Fernandes, A. D., Reid, J. N., Macklaim, J. M., McMurrough, T. A., Edgell, D. R., and Gloor, G. B. (2014). Unifying the analysis of high-throughput sequencing datasets: characterizing rna-seq, 16s rrna gene sequencing and selective growth experiments by compositional data analysis. *Microbiome*, **2**(1), 15.

Fukuyama, J., Rumker, L., Sankaran, K., Jeganathan, P., Dethlefsen, L., Relman, D. A., and Holmes, S. P. (2017). Multidomain analyses of a longitudinal human microbiome intestinal cleanout perturbation experiment. *PLoS computational biology*, **13**(8), e1005706.

Gavin, P., Mullaney, J., Loo, D., Lê Cao, K.-A., Gottlieb, P., Hill, M., Zipris, D., and Hamilton-Williams, E. (2018). Intestinal metaproteomics reveals host-microbiota interactions in subjects at risk for type 1 diabetes. *DIABETES CARE*, **41**, 2178–2186.

Gerber, G. K., Onderdonk, A. B., and Bry, L. (2012). Inferring dynamic signatures of microbes in complex host ecosystems. *PLoS computational biology*, **8**(8), e1002624.

Gloor, G. B., Macklaim, J. M., Pawlowsky-Glahn, V., and Egozcue, J. J. (2017). Microbiome datasets are compositional: and this is not optional. *Frontiers in microbiology*, **8**, 2224.

Grice, E. A. and Segre, J. A. (2011). The skin microbiome. *Nature Reviews Microbiology*, **9**(4), 244.

Guidi, L., Chaffron, S., Bittner, L., Eveillard, D., Larhlimi, A., Roux, S., Darzi, Y., Audic, S., Berline, L., Brum, J. R., *et al.* (2016). Plankton networks driving carbon export in the oligotrophic ocean. *Nature*, **532**(7600), 465.

Hoyos-Hernandez, C., Hoffmann, M., Guenne, A., and Mazeas, L. (2014). Elucidation of the thermophilic phenol biodegradation pathway via benzoate during the anaerobic digestion of municipal solid waste. *Chemosphere*, **97**, 115–119.

Huang, D.-S. and Zheng, C.-H. (2006). Independent component analysis-based penalized discriminant method for tumor classification using gene expression data. *Bioinformatics*, **22**(15), 1855–1862.

Jacques, J. and Preda, C. (2014). Functional data clustering: a survey. *Advances in Data Analysis and Classification*, **8**(3), 231–255.

Jolliffe, I. (2005). *Principal component analysis*. Wiley Online Library.

Knight, R., Jansson, J., Field, D., Fierer, N., Desai, N., Fuhrman, J. A., Hugenholtz, P., Van Der Lelie, D., Meyer, F., Stevens, R., *et al.* (2012). Unlocking the potential of metagenomics through replicated experimental design. *Nature biotechnology*, **30**(6), 513.

Kunin, V., Engelbrektson, A., Ochman, H., and Hugenholtz, P. (2010). Wrinkles in the rare biosphere: pyrosequencing errors can lead to artificial inflation of diversity estimates. *Environmental microbiology*, **12**(1), 118–123.

Lê Cao, K., Rossouw, D., Robert-Granié, C., Besse, P., *et al.* (2008). A sparse PLS for variable selection when integrating omics data. *Statistical applications in genetics and molecular biology*, **7**, Article–35.

Limam, I., Guenne, A., Driss, M. R., and Mazéas, L. (2010). Simultaneous determination of phenol, methylphenols, chlorophenols and bisphenol-a by headspace solid-phase microextraction-gas chromatography-mass spectrometry in water samples and industrial effluents. *International Journal of Environmental and Analytical Chemistry*, **90**(3-6), 230–244.

Luo, D., Ziebell, S., and An, L. (2017). An informative approach on differential abundance analysis for time-course metagenomic sequencing data. *Bioinformatics*, **33**(9), 1286–1292.

Lê Cao, K.-A., Costello, M.-E., Lakis, V. A., Bartolo, F., Chua, X.-Y., Brazeilles, R., and Rondeau, P. (2016a). Mixmc: a multivariate statistical framework to gain insight into microbial communities. *PloS one*, **11**(8), e0160169.

Lê Cao, K.-A., Costello, M.-E., Chua, X.-Y., Brazeilles, R., and Rondeau, P. (2016b). Mixmc: Multivariate insights into microbial communities. *PLoS ONE*, **11**(8), e0160169.

Madigou, C., Lê Cao, K.-A., Bureau, C., Mazéas, L., Déjean, S., and Chapleur, O. (2019). Ecological consequences of abrupt temperature changes in anaerobic digesters. *Chemical Engineering Journal*, **361**, 266–277.

Metwally, A. A., Yang, J., Ascoli, C., Dai, Y., Finn, P. W., and Perkins, D. L. (2018). Metalonda: a flexible r package for identifying time intervals of differentially abundant features in metagenomic longitudinal studies. *Microbiome*, **6**(1), 32.

Morris, A., Paulson, J. N., Talukder, H., Tipton, L., Kling, H., Cui, L., Fitch, A., Pop, M., Norris, K. A., and Ghedin, E. (2016). Longitudinal analysis of the lung microbiota of cynomolgous macaques during long-term shiv infection. *Microbiome*, **4**(1), 38.

Palmer, C., Bik, E. M., DiGiulio, D. B., Relman, D. A., and Brown, P. O. (2007). Development of the human infant intestinal microbiota. *PLoS biology*, **5**(7), e177.

Paulson, J. N., Talukder, H., and Bravo, H. C. (2017). Longitudinal differential abundance analysis of microbial marker-gene surveys using smoothing splines. *BioRxiv*, page 099457.

Poirier, S. and Chapleur, O. (2018). Inhibition of anaerobic digestion by phenol and ammonia: Effect on degradation performances and microbial dynamics. *Data in brief*, **19**, 2235–2239.

Poirier, S., Desmond-Le Quéméner, E., Madigou, C., Bouchez, T., and Chapleur, O. (2016). Anaerobic digestion of biowaste under extreme ammonia concentration: identification of key microbial phylotypes. *Bioresource technology*, **207**, 92–101.

Ramsay, J. and Silverman, B. (2005). Functional data analysis. 2nd springer. *New York*.

Ribicic, D., McFarlin, K. M., Netzer, R., Brakstad, O. G., Winkler, A., Throne-Holst, M., and Størseth, T. R. (2018). Oil type and temperature dependent biodegradation dynamics-combining chemical and microbial community data through multivariate analysis. *BMC microbiology*, **18**(1), 83.

Ridenhour, B. J., Brooker, S. L., Williams, J. E., Van Leuven, J. T., Miller, A. W., Dearing, M. D., and Remien, C. H. (2017). Modeling time-series data from microbial communities. *The ISME journal*, **11**(11), 2526.

Rohart, F., Gautier, B., Singh, A., and Lê Cao, K.-A. (2017). mixomics: an r package for 'omics feature selection and multiple data integration. *PLoS Computational Biology*, **13**(11).

Rousseeuw, P. J. (1987). Silhouettes: a graphical aid to the interpretation and validation of cluster analysis. *Journal of computational and applied mathematics*, **20**, 53–65.

Ruppert, D. (2002). Selecting the number of knots for penalized splines. *Journal of computational and graphical statistics*, **11**(4), 735–757.

Rutayisire, E., Huang, K., Liu, Y., and Tao, F. (2016). The mode of delivery affects the diversity and colonization pattern of the gut microbiota during the first year of infants' life: a systematic review. *BMC gastroenterology*, **16**(1), 86.

Shields-Cutler, R. R., Al-Ghalith, G. A., Yassour, M., and Knights, D. (2018). Splinectomer enables group comparisons in longitudinal microbiome studies. *Frontiers in microbiology*, **9**, 785.

Shin, H., Pei, Z., Martinez, K. A., Rivera-Vinas, J. I., Mendez, K., Cavallin, H., and Dominguez-Bello, M. G. (2015). The first microbial environment of infants born by c-section: the operating room microbes. *Microbiome*, **3**(1), 59.

Singh, A., Gautier, B., Shannon, C., Rohart, F., Vacher, M., S, T., and Lê Cao, K.-A. (2019). Diablo: an integrative approach for identifying key molecular drivers from multi-omic assays. *Bioinformatics*, **bty1054**.

Smith, C. A., Want, E. J., O'Maille, G., Abagyan, R., and Siuzdak, G. (2006). Xcms: processing mass spectrometry data for metabolite profiling using nonlinear peak alignment, matching, and identification. *Analytical chemistry*, **78**(3), 779–787.

Straube, J., Gorse, AD, P., Huang, B., and Lê Cao, K.-A. (2015). A linear mixed model spline framework for analysing time course omics data. *PLoS ONE*.

Straube, J., Lê Cao, K.-A., and Huang, E. (2016). *lmms: Linear Mixed Effect Model Splines for Modelling and Analysis of Time Course Data*. R package version 1.3.3.

Straube, J., Huang, B. E., and Lê Cao, K.-A. (2017). Dynomics to identify delays and co-expression patterns across time course experiments. *Scientific reports*, **7**, 40131.

Tenenhaus, A. and Tenenhaus, M. (2011). Regularized generalized canonical correlation analysis. *Psychometrika*, **76**(2), 257–284.

Tenenhaus, A., Philippe, C., Guillemot, V., Le Cao, K.-A., Grill, J., and Frouin, V. (2014). Variable selection for generalized canonical correlation analysis. *Biostatistics*, **15**(3), 569–83.

Thursby, E. and Juge, N. (2017). Introduction to the human gut microbiota. *Biochemical Journal*, **474**(11), 1823–1836.

Tibshirani, R. (1996). Regression shrinkage and selection via the lasso. *Journal of the Royal Statistical Society. Series B (Methodological)*, pages 267–288.

Torres, B., Porras, G., García, J. L., and Díaz, E. (2003). Regulation of the mhp cluster responsible for 3-(3-hydroxyphenyl) propionic acid degradation in escherichia coli. *Journal of Biological Chemistry*.

Verbyla, A. P., Cullis, B. R., Kenward, M. G., and Welham, S. J. (1999). The analysis of designed experiments and longitudinal data by using smoothing splines. *Journal of the Royal Statistical Society: Series C (Applied Statistics)*, **48**(3), 269–311.

Watkins, P. A., Moser, A. B., Toomer, C. B., Steinberg, S. J., Moser, H. W., Karaman, M. W., Ramaswamy, K., Siegmund, K. D., Lee, D. R., Ely, J. J., *et al.* (2010). Identification of differences in human and great ape phytanic acid metabolism that could influence gene expression profiles and physiological functions. *BMC physiology*, **10**(1), 19.

Witten, D. M., Tibshirani, R., and Hastie, T. (2009). A penalized matrix decomposition, with applications to sparse principal components and canonical correlation analysis. *Biostatistics*, **10**(3), 515–534.

Wold, H. (1975). *Path models with latent variables: The NIPALS approach*. Acad. Press.

A   Linear Mixed Model Splines (LMMS) models

The first model assumes the response is a straight line not affected by individual variation. Let $y_{ij}(t_{ij})$ be the taxa normalised count for individual (or biological replicate) i at time t_{ij}, where $i = 1, 2, ..., n$, $j = 1, 2, ..., m_i$, N is the sample size and m_i is the number of observations for individual i for the given taxa. A simple linear regression of abundance $y_{ij}(t_{ij})$ on time t_{ij}, with the intercept β_0 and slope β_1 is estimated via ordinary least squares:

$$y_{ij}(t_{ij}) = \beta_0 + \beta_1 t_{ij} + \epsilon_{ij}, \quad \text{where} \quad \epsilon_{ij} \quad \sim \quad N(0, \sigma_\epsilon^2). \tag{1}$$

As nonlinear response patterns are commonly encountered, a second model uses a spline truncated line basis as proposed by Durban Durbán *et al.* (2005) to model a curve:

$$y_{ij}(t_{ij}) = f(t_{ij}) + \epsilon_{ij}, \quad \text{where} \quad \epsilon_{ij} \sim N(0, \sigma_\epsilon^2), \tag{2}$$

where f represents a penalized spline which depends on a set of knot positions $\kappa_1, ..., \kappa_K$ in the range of $\{t_{ij}\}$, some unknown coefficients u_k, an intercept β_0 and a slope β_1, i.e.

$$f(t_{ij}) = \beta_0 + \beta_1 t_{ij} + \sum_{k=1}^{K} u_k(t_{ij} - \kappa_k)_+,$$

$$\text{with} \quad (t_{ij} - \kappa_k)_+ = \begin{cases} t_{ij} - \kappa_k & \text{if} \quad t_{ij} - \kappa_k > 0, \\ 0 & \text{otherwise.} \end{cases}$$

The choice of the number of knots K and their positions influences the flexibility of the curve. As proposed by Ruppert (2002), we estimate the number of knots based on the number of measured time points T as $K = max(5, min(\lfloor \frac{T}{4} \rfloor, 40))$, placing the knots $\kappa_1...\kappa_K$ at quantiles of the time interval of interest.

A third model accounts for individual variation in Eq. (3) with the addition of a subject-specific random effect U_i to the mean response $f(t_{ij})$. We assume $f(t_{ij})$ to be a fixed (yet unknown) population curve, U_i is treated as a random realisation from an underlying Gaussian distribution independent from the previously defined random error ϵ_{ij}. The individual curves are expected to be parallel to the mean curve as we assume the subject-specific random effects to be constant over time:

$$y_{ij}(t_{ij}) = f(t_{ij}) + U_i + \epsilon_{ij}, \quad \text{where} \quad U_i \sim N(0, \sigma_U^2). \tag{3}$$

The final and fourth model is an extension to Eq. (3) that assumes individual deviations are straight lines, where individual-specific random intercepts a_{i0} and slopes a_{i1} are fitted:

$$y_{ij}(t_{ij}) = f(t_{ij}) + a_{i0} + a_{i1} t_{ij} + \epsilon_{ij},$$

$$\text{with} \quad \epsilon_{ij} \quad \sim N(0, \sigma_\epsilon^2) \quad \text{and} \quad (a_{i0}, a_{i1})^T \sim N(0, \Sigma). \tag{4}$$

Here we assume independence between the random intercept and slope, so the covariance matrix for the random effects Σ is diagonal.